



Preparation and Characterization of Cellulose-Chitosan-Silk Fibroin Composite Films Using Lithium Bromide (LiBr) Solution

Jiwook YANG^{1,†} · Sungyeol KIM¹ · Kyojung HWANG¹ · Jaejung LEE¹

ABSTRACT

Cellulose-chitosan-silk fibroin (CCF) composite films were fabricated using a 60% lithium bromide solution, and their physicochemical properties were analyzed. The CCF films exhibited a light yellowish-beige color with high transparency, and no distinct differences were observed in their cross-sectional structures. Throughout the dissolution and regeneration processes, cellulose was converted from cellulose I to cellulose II, with chitosan and silk fibroin (SF) influencing the crystalline structure of the film. High concentrations of cellulose and chitosan inhibited the formation of well-defined β -sheet structures, resulting in a composite with mixed silk I and II conformations and hydrogen bonding among the polymers. In the dry film, the tensile strength and elongation increased with increasing SF content; however, excessive SF led to a decrease in the elastic modulus. In the wet film, both tensile strength and elongation increased with increasing SF content, with CCF9 exhibiting the highest tensile strength owing to enhanced hydrogen bonding, partial β -sheet formation in SF, and physical entanglement between polymers. The swelling ratio of the CCF films increased with SF content, particularly in physiological fluids, owing to enhanced interactions between water molecules, ions, and the hydrophilic functional groups of SF. When the SF content exceeded 60%, partial β -sheet formation and strengthened hydrogen bonding significantly improved the swelling and mechanical properties. These results demonstrate the potential of CCF films in cosmetics, food packaging, and biomaterials, particularly for tissue engineering, wound dressings, and drug delivery systems in biomedical applications.

Keywords: cellulose, chitosan, silk fibroin, composite, film, lithium bromide (LiBr)

1. INTRODUCTION

With the growing interest in bio-based materials that offer excellent biocompatibility and environmental friendliness, research on natural polymer-based composite materials has garnered significant attention. Cellulose, chitosan, starch, and silk fibroin (SF) are representative

natural polymers with low toxicity, minimal environmental impact, renewability, and biodegradability, making them highly suitable for various industries (Geyer *et al.*, 2017; Park *et al.*, 2013; Rillig, 2012; Sheavly and Register, 2007).

Cellulose is a linear polymer comprising repeating β -(1 \rightarrow 4)-glucose units. It is abundant, cost-effective, and

Date Received February 21, 2025; Date Revised February 27, 2025; Date Accepted March 10, 2025; Published March 25, 2025

¹ Forest Products and Industry Department, National Institute of Forest Science, Seoul 02455, Korea

[†] Corresponding author: Jiwook YANG (e-mail: jiwooky85@gmail.com, <https://orcid.org/0000-0002-6657-1418>)

© Copyright 2025 The Korean Society of Wood Science & Technology. This is an Open-Access article distributed under the terms of the Creative Commons Attribution Non-Commercial License (<http://creativecommons.org/licenses/by-nc/4.0/>) which permits unrestricted non-commercial use, distribution, and reproduction in any medium, provided the original work is properly cited.

exhibits remarkable physicochemical properties, such as biocompatibility, water absorbency, and biodegradability, facilitating its use across diverse material industries (Feng and Chen, 2008; Fink *et al.*, 2001; Gwak *et al.*, 2022; Jullaprom *et al.*, 2025; Kim *et al.*, 2017a; Marsano *et al.*, 2007; Mawardi *et al.*, 2025; Seo and Kim, 2024; Setyayunita *et al.*, 2022; Zhou *et al.*, 2013). However, the strong intra- and intermolecular hydrogen bonding of cellulose results in a highly crystalline structure, making it insoluble in water and most organic solvents. Therefore, several solvents, including *N,N*-dimethylacetamide/lithium chloride, *N*-methyl-morpholine-*N*-oxide, dimethyl sulfoxide/tetrabutylammonium fluoride, dinitrogen tetroxide/dimethylformamide, sodium hydroxide (NaOH)/urea, ionic liquids, and lithium bromide (LiBr) aqueous solutions, have been developed for cellulose dissolution systems (Feng and Chen, 2008; Gwak *et al.*, 2024; Kim *et al.*, 2017b; Yang *et al.*, 2014a; Zhou *et al.*, 2013).

Chitosan, a natural polymer obtained by deacetylating chitin derived from crustaceans, such as shrimp and crabs, or from fungi and insects, shares structural similarity with cellulose. It is non-toxic, biocompatible, biodegradable, and non-immunogenic, making it widely applicable in textiles, paper manufacturing, agriculture, and food production. Its antimicrobial properties, wound-healing capabilities, and body thermoregulation characteristics make it particularly valuable in medical applications (Abdul Khalil *et al.*, 2016; He *et al.*, 2011; Jang and Nah, 2008; Kuzmina *et al.*, 2012; Ostadossein *et al.*, 2015; Twu *et al.*, 2003).

Yang *et al.* (2018) investigated the fabrication and physicochemical properties of cellulose-chitosan composite materials. While these films are eco-friendly and biodegradable, they exhibit inherent limitations in mechanical strength and flexibility when used alone. To overcome these limitations, recent studies have actively explored strategies to incorporate various polymers to enhance material properties and introduce novel functionalities (Dungani *et al.*, 2022; Sionkowska, 2011;

Zhou *et al.*, 2013).

Silk proteins produced by silkworms and spiders primarily comprise fibroin and sericin, with fibroin serving as the main structural protein. Fibroin is hydrophobic and exhibits outstanding mechanical strength, oxygen and moisture barrier properties, biocompatibility, and biodegradability. Thus, it is suitable for various applications, including food packaging, cosmetics, enzyme immobilization supports, cell culture scaffolds, and biomedical materials (Bhardwaj and Kundu, 2011; Cho *et al.*, 2014; Kim *et al.*, 2017a; Noishiki *et al.*, 2002). In particular, SF forms a unique molecular structure incorporating β -sheet arrangements, which contributes to its exceptional mechanical strength and flexibility. Moreover, its excellent compatibility with other functional materials enables its broad application in the development of high-performance bio-based materials.

In this study, we investigated the structural and physical properties of a cellulose-chitosan composite matrix reinforced with SF. We systematically analyzed changes in microstructure, mechanical strength, elongation, and moisture resistance with varying SF content. Additionally, we investigated the interaction mechanisms between the components to optimize the composite material.

2. MATERIALS and METHODS

2.1. Materials

Alpha-cellulose (Sigma-Aldrich, St. Louis, MO, USA) and chitosan (MW 190–310 kDa, deacetylation degree greater than 75%; Sigma-Aldrich) were used as the primary materials in this study. SF obtained from silkworm cocoons (*Bombyx mori*) was provided by Chunzam Bio (Seoul, Korea). Sodium carbonate (Na₂CO₃; Daejung Chemicals & Metals, Siheung, Korea) was used for silk degumming. LiBr from Samchun Pure Chemical (Pyeongtaek, Korea) was used as the solvent for polymer dissolution.

2.2. Experimental methods

2.2.1. Preparation of the cellulose-chitosan-silk fibroin composite film

SF was prepared by degumming silkworm cocoons in a 0.5 wt% Na₂CO₃ aqueous solution at 90 ± 1°C for 4 h. Degummed silk was rinsed five times with distilled water and subsequently dried in an oven at 60 ± 1°C for 24 h (Kim *et al.*, 2017a; Shang *et al.*, 2011; Zhou *et al.*, 2013).

A 60 wt% LiBr solution was prepared as the solvent. To prepare the cellulose-chitosan composite solution, 1 g of cellulose and chitosan (at an 8:2 mass ratio) was dissolved in 89 g of 60% LiBr solution and stirred at 145 ± 1°C for 5 min. Subsequently, an SF solution was added to the mixture and stirred for 2 min to ensure homogeneous blending.

The SF solution was prepared by dissolving solid SF in 10 g of LiBr solution, adjusting the SF content to 0, 30, 60, or 90 wt% based on 1 g of the cellulose-chitosan mixture. To completely dissolve SF, the solution was heated in a drying oven at 70 ± 1°C for 4 h before use.

The resulting homogeneous solutions were cast onto preheated glass plates at 90°C and subsequently cooled to room temperature for regeneration. The regenerated gels were washed under running water for 1 day, pressed for 30 min to remove excess water, and dried in an oven

at 105 ± 1°C for 24 h to obtain the cellulose-chitosan-silk fibroin (CCF) composite films (Fig. 1).

The films were named CCF0, CCF3, CCF6, and CCF9 according to their SF content ratios.

2.2.2. Characterization of the cellulose-chitosan-silk fibroin composite film

The cross-sectional structures of the CCF composite films were observed using scanning electron microscopy (SEM; EM-30 MiniSEM, COXEM, Daejeon, Korea). The samples were cryo-fractured using liquid nitrogen to observe the cut sides. The X-ray diffraction (XRD) patterns of the CCF films were obtained using an X'Pert PRO MPD X-ray diffractometer (PANalytical, EA Almelo, The Netherlands). Fourier-transform infrared (FT-IR) spectra of the films were obtained using a Vertex70 spectrometer (Bruker Optics, Ettlingen, Germany) equipped with an attenuated total reflection accessory. A universal testing machine (TO-102D, Test One, Siheung, Korea) was used to determine the mechanical properties of the films, including tensile strength, elongation at break, and elastic modulus. Film samples (15 × 60 mm) were tested, and the average of three measurements was reported. The mechanical behavior of the films was examined under both dry and wet conditions. In the wet state, the film was soaked in water for 30 min, followed by the removal of excess water

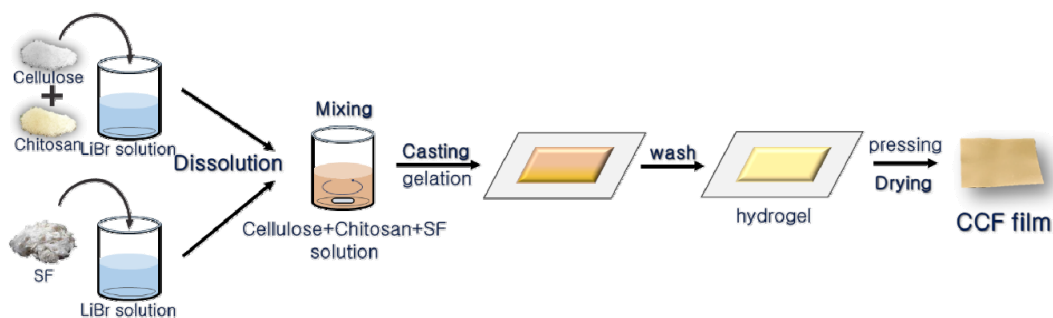


Fig. 1. Preparation of the cellulose-chitosan-silk fibroin (CCF) composite film. SF: silk fibroin, LiBr: lithium bromide.

and storage in a polypropylene bag. The swelling properties of the CCF films in water and physiological fluids were analyzed. The film was cut into a size of 10(W) × 30(L) mm and used, and the prepared samples were impregnated with water and physiological solution at 37 ± 1°C for 12 h; subsequently, the weight was measured. For the physiological fluids, sodium chloride (NaCl; 9 g NaCl dissolved in 1,000 mL distilled water) and urea (25 g urea in 500 mL distilled water) solutions were prepared and used.

3. RESULTS and DISCUSSION

3.1. Morphology of the cellulose-chitosan-silk fibroin composite film

Fig. 2 shows photographs of the CCF composite films prepared with varying SF ratios in a 60% LiBr solution.

All CCF films exhibited high transparency, and the

text beneath them was clearly visible. CCF0, which lacked SF, exhibited a light yellowish-beige color owing to the presence of chitosan. In a previous study (Yang *et al.*, 2018), films solely comprising cellulose were transparent, whereas the addition of chitosan resulted in a darker coloration. The same result was observed for CCF0. In contrast, the color of CCF3, CCF6, and CCF9 progressively darkened with increasing SF content. Pure SF exhibits a pale-yellow color owing to the presence of β -sheet structures and amino acids such as tyrosine, phenylalanine, and tryptophan within the fibroin molecular chains (Perotto *et al.*, 2017; Santos *et al.*, 2019; Yasunaga *et al.*, 2023). Therefore, the proportion of β -sheet structures and amino acids increases with increasing SF content in the CCF films, resulting in a darker color. Additionally, changes in intermolecular hydrogen bonding and structural density may contribute to variations in color.

Fig. 3 shows the cross-sectional images of the CCF

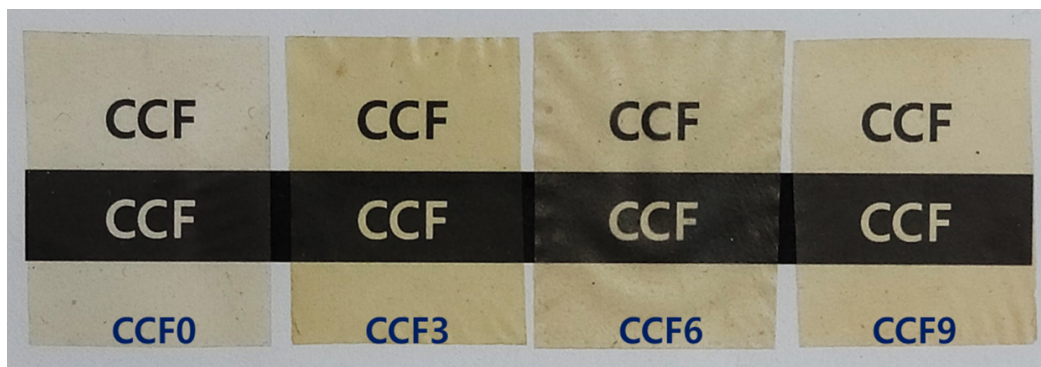


Fig. 2. Photographs of the cellulose-chitosan-silk fibroin (CCF) films according to the silk fibroin ratios.

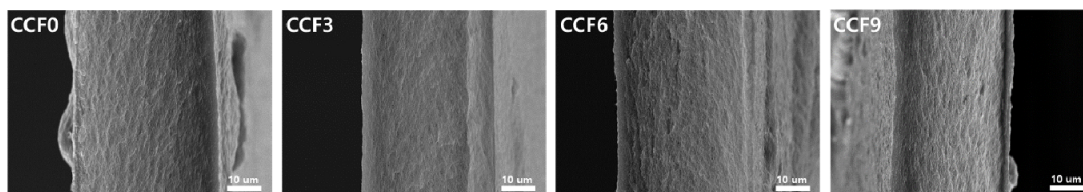


Fig. 3. Scanning electron microscopy images of cross-sections of cellulose-chitosan-silk fibroin (CCF) films with different silk fibroin ratios (× 2,500).

films obtained using SEM. The cross-sections of all CCF films displayed a similar structure with a slightly rough texture, showing no significant changes with increasing SF content.

3.2. X-ray diffraction analysis

Fig. 4 shows the XRD results for CCF films with varying SF contents. In a previous study (Yang *et al.*, 2020), which employed the same film fabrication method as in this study, the XRD patterns of cellulose films exhibited peaks at $2\theta = 20.2^\circ$ and 22.8° , indicating that the crystalline structure of α -cellulose, used as a raw material, transformed from cellulose I to II throughout the dissolution and regeneration processes in the LiBr aqueous solution. In the XRD pattern of α -cellulose, peaks attributed to the crystalline structure of cellulose I were observed at $2\theta = 14.8^\circ$, 16.4° , 22.4° , and 34.6° . However, in CCF0, these peaks shifted to $2\theta = 20.4^\circ$ and 22.8° , indicating that the crystalline structure underwent a transformation from cellulose I to II during dissolution and regeneration (Cheng *et al.*, 2012; Lee *et al.*, 2022; Oh *et al.*, 2005; Yang *et al.*, 2014b; Zhou *et al.*, 2013).

Additionally, as chitosan in CCF0 was also dissolved

and regenerated, the peaks of α -chitosan at $2\theta = 11.1^\circ$ and 19.9° disappeared (Li *et al.*, 2001). The regenerated cellulose peak at $2\theta = 20.2^\circ$ overlapped with the regenerated chitosan peak at 20.2° , slightly shifting it to 20.4° . This suggests that, during dissolution in the LiBr aqueous solution, chitosan macromolecules lost their crystalline structure and existed in a random coil state. Intermolecular hydrogen bonding occurred between the dissolved cellulose and chitosan chains, leading to molecular rearrangement and the formation of a new crystalline structure in the film. Furthermore, a diffraction peak at $2\theta = 12.3^\circ$, attributed to the crystalline regions of chitosan, was observed in CCF0 and all other CCF films (Antonino *et al.*, 2017; Fu *et al.*, 2017; Kim *et al.*, 2017b; Lu *et al.*, 2004; Ma *et al.*, 2015; Weng *et al.*, 2017).

In the XRD pattern of SF, the characteristic peak of silk I was observed at $2\theta = 28.8^\circ$, whereas that corresponding to silk II appeared at $2\theta = 20.5^\circ$, indicating the presence of the typical crystalline structure of natural SF fibers. However, in CCF3, CCF6, and CCF9, no peaks corresponding to the crystalline structure of silk II were observed, suggesting that the incorporation of SF did not induce sufficient β -sheet formation to significantly affect the crystalline structure. This suggests that, during dis-

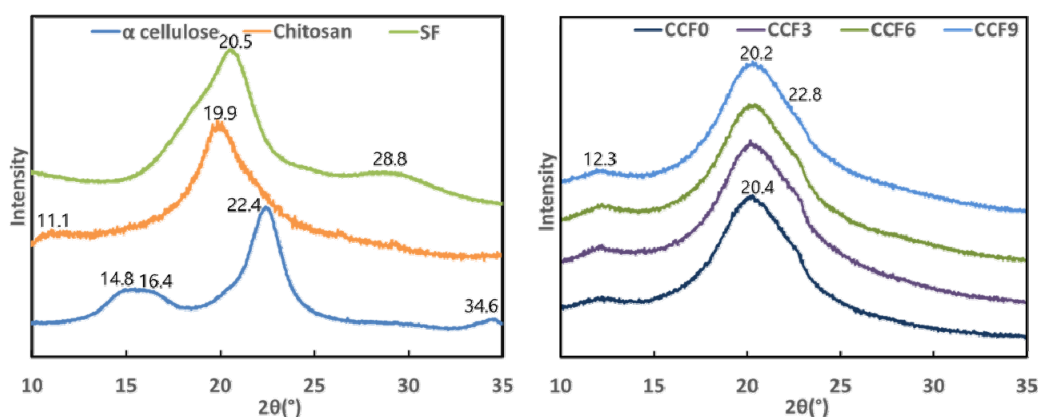


Fig. 4. X-ray diffraction patterns of α -cellulose, chitosan, silk fibroin (SF), and cellulose-chitosan-silk fibroin (CCF) films with different SF ratios.

solution in the LiBr aqueous solution, the crystalline structure of silk I in SF was disrupted, forming a random coil conformation. Subsequently, during the regeneration process, SF did not develop a well-defined β -sheet structure, as it was immobilized in a gel-like form with the highly concentrated cellulose and chitosan.

With the addition of SF, the peak shifted slightly from $2\theta = 20.4^\circ$ to 20.2° , and the peak intensity increased. This indicates that the random coil structure of SF induces changes in physical interactions, such as hydrogen bonding and polymer entanglement, which affect the overall crystalline structure of the film. This suggests that the dissolved cellulose, chitosan, and SF were thoroughly and uniformly mixed during the dissolution process (Cao and Wang, 2009; Chen *et al.*, 2012; Cheng *et al.*, 2012; Guang *et al.*, 2015; Kim *et al.*, 2017a; Li *et al.*, 2001; Marsano *et al.*, 2008; Moraes *et al.*, 2010; Wang *et al.*, 2019; Yang *et al.*, 2014b; Zhang *et al.*, 2013).

3.3. Fourier-transform infrared analysis

Fig. 5 shows the FTIR spectra of the CCF composite films. All CCF films exhibited characteristic peaks associated with amorphous cellulose at 1,365 (C-H bending), 1,155 (C-O-C stretching), 1,022 (C-O vibration), and

898 cm^{-1} (β -glycosidic linkages; Hoang *et al.*, 2021; Oliveira Barud *et al.*, 2015; Park *et al.*, 2022; Suryanto *et al.*, 2024; Zhang *et al.*, 2018). Chitosan exhibited similar peaks owing to its polysaccharide structure, leading to peak overlap with cellulose (Anicuta *et al.*, 2010; Moraes *et al.*, 2010; Yang *et al.*, 2020). In a previous study (Yang *et al.*, 2018), the FT-IR spectrum of a pure cellulose film exhibited a peak at $3,369 \text{ cm}^{-1}$ corresponding to the OH group. However, upon chitosan incorporation, this peak shifted to $3,357 \text{ cm}^{-1}$ in CCF0. Additionally, the presence of chitosan introduced a weak peak at $1,591 \text{ cm}^{-1}$, attributed to NH bending of amide II. This shift and peak emergence are attributed to hydrogen bonding interactions between cellulose (-OH groups) and chitosan (-OH and $-\text{NH}_2$ groups) during the mixing and regeneration processes (Anicuta *et al.*, 2010; de Souza Costa-Júnior *et al.*, 2009; Lin *et al.*, 2012; Nawawi *et al.*, 2023; Negrea *et al.*, 2015; Weng *et al.*, 2017).

In the CCF film, as SF was mixed, the peak at $1,533 \text{ cm}^{-1}$ due to NH bending of amide II of SF and those corresponding to C = O stretching of amide I appeared at $1,625$ and $1,652 \text{ cm}^{-1}$, respectively. Additionally, the intensity of these peaks tended to increase with increasing SF content in the films. In particular, the peak at $1,625 \text{ cm}^{-1}$ is a characteristic peak derived from

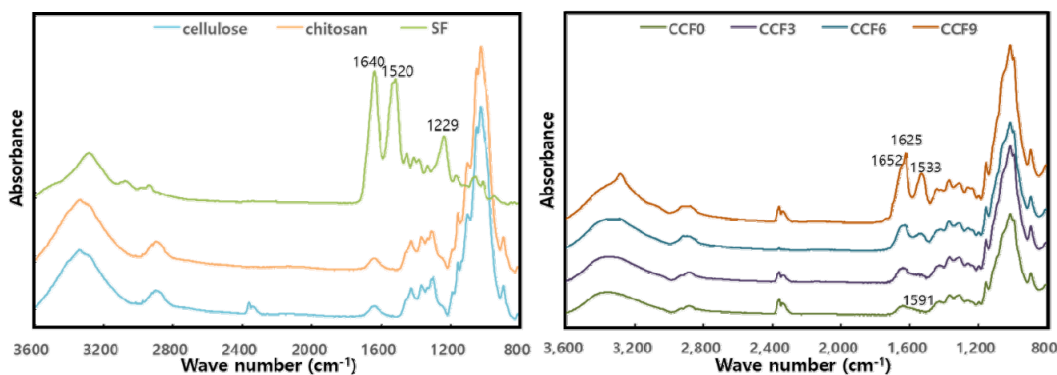


Fig. 5. Fourier-transform infrared spectra of the cellulose-chitosan-silk fibroin (CCF) films with different silk fibroin (SF) ratios.

β -sheet structures (silk II), indicating that some β -sheet crystal structures formed in the CCF film as SF ratio increased, resulting in a composite structure mixed with crystal structures of silk I and II. The β -sheet crystal structure of SF was not identified in the XRD results. However, although the β -sheet structure was not sufficiently formed to affect the crystal structure, some crystal structure of silk II developed inside the film with increasing SF content.

In the region of 3,600–3,000 cm^{-1} , with increasing SF content, the peak at 3,357 cm^{-1} in CCF0 slightly shifted, and its intensity increased. These hydrogen bonding interactions occur between the carbonyl ($\text{C} = \text{O}$) and NH groups of SF and hydroxyl (OH) and amine (NH_2) groups in cellulose and chitosan. These interactions suggested that molecular-level hydrogen bonding occurred during dissolution and regeneration. Furthermore, in CCF9, which contained the highest SF content, an additional peak appeared at 3,280 cm^{-1} , corresponding to regenerated SF-NH groups (Anicuta *et al.*, 2010; Chen *et al.*, 2012; Fu *et al.*, 2017; Guang *et al.*, 2015; Moraes *et al.*, 2010).

3.4. Mechanical analysis

Table 1 presents the thicknesses of the CCF composite films in the dry and wet states. In the dry state, the film thickness did not vary significantly with the addition of SF. However, in the wet state, the difference in thickness between the dry and wet films increased with increasing SF content. This phenomenon is attributed to the increase in the number of hydrophilic groups of SF, which leads to enhanced water absorption and swelling.

The mechanical properties of the CCF composite films, including the tensile strength, elongation, and elastic modulus, were evaluated in the dry and wet states based on the SF mixing ratio. Fig. 6 shows the mechanical properties of CCF films in the dry state. The tensile strengths of CCF0, CCF3, CCF6, and CCF9 were 84.86, 88.47, 101.18, and 102.57 MPa, respectively, indicating a gradual increase with increasing SF content. The elongation values of the CCF films were 2.40%, 3.15%, 3.64%, and 3.12%, while the elastic moduli were 3.48, 3.77, 3.28, and 3.04 GPa, respectively, indicating that these values increased and subsequently decreased with increasing SF content.

Table 1. Thickness of the cellulose-chitosan-silk fibroin (CCF) films in dry and wet states (unit: μm)

Film state	CCF0	CCF 3	CCF 6	CCF 9
Dry	43.1 \pm 3.3	45.5 \pm 4.3	45.5 \pm 4.3	43.2 \pm 0.9
Wet	59.8 \pm 2.3	66.5 \pm 4.2	66.4 \pm 2.4	66.5 \pm 1.9

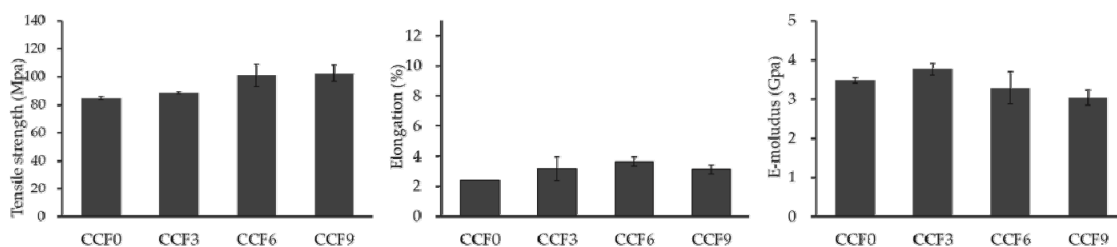


Fig. 6. Tensile strength, elongation, and elastic moduli of dry-state cellulose-chitosan-silk fibroin (CCF) films depending on the silk fibroin ratios.

With the addition of SF, intermolecular interactions, such as hydrogen bonding between cellulose, chitosan, and SF polymers, occur, improving the mechanical properties of the dried CCF film (Zhang *et al.*, 2014). Additionally, the physical entanglement of the polymer chains contributed to this enhancement. The crystalline regions of polymers efficiently absorb energy and withstand deformation, whereas the amorphous regions cause the polymer chains to intertwine more closely, thereby strengthening the film (Dorishetty *et al.*, 2020; Liu *et al.*, 2016; Zhang *et al.*, 2014).

However, excessive SF content can lead to intramolecular rather than intermolecular hydrogen bonding, causing phase separation and reducing the uniformity of the polymer matrix. Consequently, the cohesive force between the polymer matrix and filler weakens, leading to a decrease in mechanical strength (Fu *et al.*, 2017; Shang *et al.*, 2011; Shih *et al.*, 2009; Xu *et al.*, 2005; Yao *et al.*, 2015).

Fig. 7 shows the mechanical properties of the CCF composite films in the wet state. The tensile strength of the wet films decreased significantly compared with that of the dry films owing to the plasticizing effect of the absorbed water, which disrupted intermolecular interactions within the polymer matrix (Wu *et al.*, 2014).

The tensile strengths of CCF0, CCF3, CCF6, and CCF9 in the wet state were 8.40, 7.84, 8.45, and 12.48 MPa, respectively. While the tensile strength remained relatively stable regardless of the SF content, it exhi-

bited a significant increase in CCF9. The elongations at break for the wet films were 4.66%, 4.22%, 5.85%, and 9.81%, indicating an increasing trend with increasing SF content. The elastic moduli increased with increasing SF content, with values of 0.17, 0.15, 0.15, and 0.13 GPa, respectively.

Water molecules absorbed by the film interfere with the interaction between the polymers, thereby weakening the binding force. Nevertheless, the tensile strength increases in the wet state with increasing SF content as the bonding strength between the polymers improves with increasing number of hydrogen bonds. Additionally, the partial formation of β -sheet structures in SF contributes to improved crystallinity, which enhances the mechanical strength of the film. This is because the main random coil structure of SF promotes physical entanglement between cellulose and chitosan, which are linear polymers, thereby improving the network stability. Finally, this increased physical entanglement likely improves elongation by inhibiting the loosening of the polymer chain, thereby increasing the resistance to shear force (Adel *et al.*, 2014; Plaza *et al.*, 2008). In particular, the greater elasticity of SF in the wet state than in the dry state influenced the strength characteristics of the wet CCF film. Additionally, insufficient development of the silk II structure in SF likely affects the mechanical strength of the composite film in a wet environment (Aytemiz *et al.*, 2018; Plaza *et al.*, 2008).

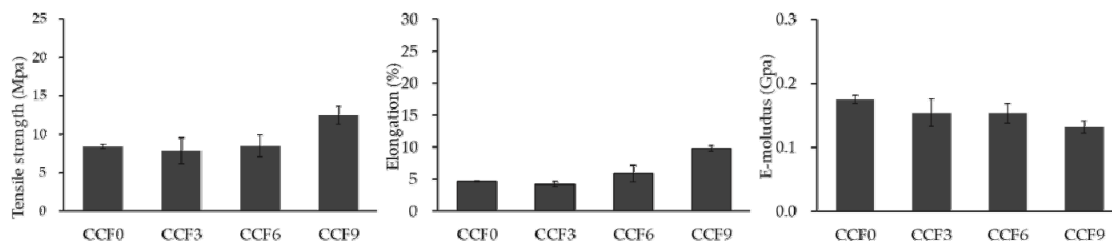


Fig. 7. Tensile strength, elongation, and elastic moduli of wet-state cellulose-chitosan-silk fibroin (CCF) films depending on the silk fibroin ratios.

3.5. Swelling analysis

Fig. 8 shows the swelling properties of the CCF composite films in water and physiological fluids. With increasing SF content, the water absorption rate of the CCF films increased slightly or showed similar results. This is because with increasing SF content in the film, the hydrogen bond between the polymers is strengthened owing to the increase in the hydroxyl, amide, and carboxyl functional groups of the fibroins, and the network density increases with increasing physical entanglement. Consequently, water cannot easily penetrate into the film; however, simultaneously, the water absorption capacity of fibroins is partially supplemented by the hydrophilic functional groups. Consequently, despite the increase in the SF content, the overall water absorption rate remained relatively stable or only slightly increased.

In contrast, the absorption rate of the CCF film in the NaCl solution was higher than that in water, and the rate of increase in absorption also exhibited a greater trend with increasing SF content. This can be attributed to electrostatic interactions between Na^+ and Cl^- ions and the amino acids present in fibroin, which facilitated the diffusion of ions and water into the film matrix. With increasing SF content, the electrostatic interactions within the polymer network increased, enabling the diffusion of more ions and water into the film.

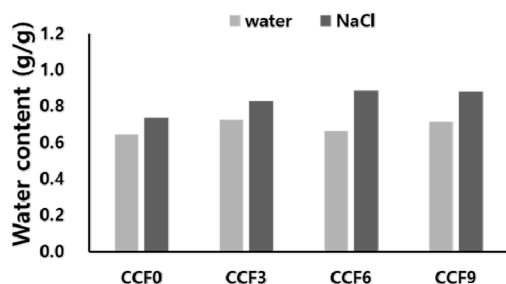


Fig. 8. Effects of water and the physiological fluid (NaCl solution) on the swelling ratio of cellulose-chitosan-silk fibroin (CCF) films.

4. CONCLUSIONS

In this study, CCF composite films were fabricated using a 60% LiBr solution, and their physicochemical properties were investigated. All CCF films exhibited a light yellowish-white color with high transparency, and the film color darkened with increasing SF content in the CCF film. No distinct differences were observed in the cross-sectional structures. During the dissolution and regeneration processes, cellulose I was transformed into a cellulose II crystal structure, and the presence of chitosan and SF influenced the crystalline structure of the films. The high concentrations of cellulose and chitosan hindered the formation of a well-defined β -sheet structure in SF, resulting in a composite structure with mixed silk I and II conformations. Intermolecular hydrogen bonds were formed among the three polymers.

Considering the mechanical properties of the CCF films, the tensile strength and elongation at break increased with increasing SF content in the dry state. However, excessive SF incorporation decreased the e-modulus. In the wet state, both the tensile strength and elongation increased with increasing SF content, and the tensile strength of the CCF9 sample was the highest. This is ascribed to the enhancement of hydrogen bonds, partial formation of β -sheet structures in SF, and physical entanglement between polymers. The swelling properties of the CCF films in water and physiological fluids showed a general increase in swelling ratio with increasing SF content. In particular, the swelling ratio continued to increase more prominently in physiological fluids as the interaction between water molecules and ions increased with increasing hydrophilic functional groups of SF.

Therefore, the β -sheet structure in the film was partially formed when the content ratio of SF was 60% or more, and the swelling rate and film strength increased owing to the strengthening of hydrogen bonds. This indicates the potential applicability of CCF films in various industries, such as cosmetics, food packaging,

and biomaterials. These films can potential be used in wound dressings, tissue engineering scaffolds, and drug delivery systems for biomedical applications.

CONFLICT of INTEREST

No potential conflict of interest relevant to this article was reported.

ACKNOWLEDGMENT

This study was supported by the National Institute of Forest Science (grant number: FP0700-2022-01-2025).

REFERENCES

- Abdul Khalil, H.P.S., Saurabh, C.K., Adnan, A.S., Nurul Fazita, M.R., Syakir, M.I., Davoudpour, Y., Rafatullah, M., Abdullah, C.K., Haafiz, M.K.M., Dungani, R. 2016. A review on chitosan-cellulose blends and nanocellulose reinforced chitosan bio-composites: Properties and their applications. *Carbohydrate Polymers* 150: 216-226
- Adel, A.M., Dupont, A.L., Abou-Yousef, H., El-Gendy, A., Paris, S., El-Shinnawy, N. 2014. A study of wet and dry strength properties of unaged and hygrothermally aged paper sheets reinforced with biopolymer composites. *Journal of Applied Polymer Science* 131(18): 9212-9224.
- Anicuta, S.G., Dobre, L., Stroescu, M., Jipa, I. 2010. Fourier transform infrared (FTIR) spectroscopy for characterization of antimicrobial films containing chitosan. *Analele Universității din Oradea Fascicula: Ecotoxicologie, Zootehnie si Tehnologii de Industrie Alimentara* 2010: 1234-1240.
- Antonino, R.S.C.M.D.Q., Fook, B.R.P.L., Lima, V.A.D.O., Rached, R.Í.D.F., Lima, E.P.N., Lima, R.J.D.S., Covas, C.A.P., Fook, M.V.L. 2017. Preparation and characterization of chitosan obtained from shells of shrimp (*Litopenaeus vannamei* Boone). *Marine Drugs* 15(5): 141.
- Aytemiz, D., Fukuda, Y., Higuchi, A., Asano, A., Nakazawa, C.T., Kameda, T., Yoshioka, T., Nakazawa, Y. 2018. Compatibility evaluation of non-woven sheet composite of silk fibroin and polyurethane in the wet state. *Polymers* 10(8): 874.
- Bhardwaj, N., Kundu, S.C. 2011. Silk fibroin protein and chitosan polyelectrolyte complex porous scaffolds for tissue engineering applications. *Carbohydrate Polymers* 85(2): 325-333.
- Cao, Y., Wang, B. 2009. Biodegradation of silk biomaterials. *International Journal of Molecular Sciences* 10(4): 1514-1524.
- Chen, J.P., Chen, S.H., Lai, G.J. 2012. Preparation and characterization of biomimetic silk fibroin/chitosan composite nanofibers by electrospinning for osteoblasts culture. *Nanoscale Research Letters* 7(1): 170.
- Cheng, G., Varanasi, P., Arora, R., Stavila, V., Simmons, B.A., Kent, M.S., Singh, S. 2012. Impact of ionic liquid pretreatment conditions on cellulose crystalline structure using 1-ethyl-3-methylimidazolium acetate. *The Journal of Physical Chemistry B* 116(33): 10049-10054.
- Cho, S.Y., Lee, M.E., Choi, Y., Jin, H.J. 2014. Cellulose nanofiber-reinforced silk fibroin composite film with high transparency. *Fibers and Polymers* 15(2): 215-219.
- de Souza Costa-Júnior, E., Pereira, M.M., Mansur, H.S. 2009. Properties and biocompatibility of chitosan films modified by blending with PVA and chemically crosslinked. *Journal of Materials Science: Materials in Medicine* 20(2): 553-561.
- Dorishetty, P., Balu, R., Athukoralalage, S.S., Greaves, T.L., Mata, J., de Campo, L., Saha, N., Zannettino, A.C.W., Dutta, N.K., Choudhury, N.R. 2020. Tunable biomimetic hydrogels from silk fibroin and nanocellulose. *ACS Sustainable Chemistry & Engineering* 8(6): 2375-2389.

- Dungani, R., Munawar, S.S., Karliati, T., Malik, J., Aditiawati, P., Sulistyono. 2022. Study of characterization of activated carbon from coconut shells on various particle scales as filler agent in composite materials. *Journal of the Korean Wood Science and Technology* 50(4): 256-271.
- Feng, L., Chen, Z. 2008. Research progress on dissolution and functional modification of cellulose in ionic liquids. *Journal of Molecular Liquids* 142(1-3): 1-5.
- Fink, H.P., Weigel, P., Purz, H.J., Ganster, J. 2001. Structure formation of regenerated cellulose materials from NMMO-solutions. *Progress in Polymer Science* 26(9): 1473-1524.
- Fu, R., Ji, X., Ren, Y., Wang, G., Cheng, B. 2017. Antibacterial blend films of cellulose and chitosan prepared from binary ionic liquid system. *Fibers and Polymers* 18(5): 852-858.
- Geyer, R., Jambeck, J.R., Law, K.L. 2017. Production, use, and fate of all plastics ever made. *Science Advances* 3(7): e1700782.
- Guang, S., An, Y., Ke, F., Zhao, D., Shen, Y., Xu, H. 2015. Chitosan/silk fibroin composite scaffolds for wound dressing. *Journal of Applied Polymer Science* 132(35): 42503.
- Gwak, K.S., Shin, J.H., Yoon, C.H., Choi, I.G. 2024. Conversion characteristics of chemical constituents in *Liriodendron tulipifera* and their influences on biomass recalcitrance during acid-catalyzed organosolv pretreatment. *Journal of the Korean Wood Science and Technology* 52(2): 101-117.
- Gwak, K.S., Yoon, C.H., Kim, J.C., Kim, J.H., Cho, Y.M., Choi, I.G. 2022. Conversion of glucose and xylose to 5-hydroxymethyl furfural, furfural, and levulinic acid using ethanol organosolv pretreatment under various conditions. *Journal of the Korean Wood Science and Technology* 50(6): 475-489.
- He, Q., Ao, Q., Gong, Y., Zhang, X. 2011. Preparation of chitosan films using different neutralizing solutions to improve endothelial cell compatibility. *Journal of Materials Science: Materials in Medicine* 22(12): 2791-2802.
- Hoang, M.T., Pham, T.D., Pham, T.T., Nguyen, M.K., Nu, D.T.T., Nguyen, T.H., Bartling, S., Van der Bruggen, B. 2021. Esterification of sugarcane bagasse by citric acid for Pb²⁺ adsorption: Effect of different chemical pretreatment methods. *Environmental Science and Pollution Research* 28(10): 11869-11881.
- Jang, M.K., Nah, J.W. 2008. Characterization of chitin and chitosan as a biomedical polymer. *Journal of the Korean Industrial and Engineering Chemistry* 19(5): 457-465.
- Jullaprom, S., Buapool, S., Wutisatwongkul, J. 2025. Exploring water hyacinth for sustainable sound absorber. *Journal of the Korean Wood Science and Technology* 53(1): 66-76.
- Kim, H.J., Yang, Y.J., Oh, H.J., Kimura, S., Wada, M., Kim, U.J. 2017a. Cellulose-silk fibroin hydrogels prepared in a lithium bromide aqueous solution. *Cellulose* 24(11): 5079-5088.
- Kim, U.J., Kim, H.J., Choi, J.W., Kimura, S., Wada, M. 2017b. Cellulose-chitosan beads crosslinked by dialdehyde cellulose. *Cellulose* 24(12): 5517-5528.
- Kuzmina, O., Heinze, T., Wawro, D. 2012. Blending of cellulose and chitosan in alkyl imidazolium ionic liquids. *International Scholarly Research Notices* 2012(1): 251950.
- Lee, E.A., Han, S.Y., Kwon, G.J., Kim, J.K., Bandi, R., Dadigala, R., Park, J.S., Park, C.W., Lee, S.H. 2022. Preparation and characterization of cellulose nanofibrils from lignocellulose using a deep eutectic solvent followed by enzymatic treatment. *Journal of the Korean Wood Science and Technology* 50(6): 436-447.
- Li, M., Lu, S., Wu, Z., Yan, H., Mo, J., Wang, L. 2001. Study on porous silk fibroin materials. I. Fine structure of freeze dried silk fibroin. *Journal of*

- Applied Polymer Science 79(12): 2185-2191.
- Lin, S., Chen, L., Huang, L., Cao, S., Luo, X., Liu, K., Huang, Z. 2012. Preparation and characterization of chitosan/cellulose blend films using $ZnCl_2 \cdot 3H_2O$ as a solvent. *BioResources* 7(4): 5488-5499.
- Liu, L., Li, L., Qing, Y., Yan, N., Wu, Y., Li, X., Tian, C. 2016. Mechanically strong and thermosensitive hydrogels reinforced with cellulose nanofibrils. *Polymer Chemistry* 7(46): 7142-7151.
- Lu, S., Song, X., Cao, D., Chen, Y., Yao, K. 2004. Preparation of water-soluble chitosan. *Journal of Applied Polymer Science* 91(6): 3497-3503.
- Ma, B., Hou, X., He, C. 2015. Preparation of chitosan fibers using aqueous ionic liquid as the solvent. *Fibers and Polymers* 16(12): 2704-2708.
- Marsano, E., Canetti, M., Conio, G., Corsini, P., Freddi, G. 2007. Fibers based on cellulose-silk fibroin blend. *Journal of Applied Polymer Science* 104(4): 2187-2196.
- Marsano, E., Corsini, P., Canetti, M., Freddi, G. 2008. Regenerated cellulose-silk fibroin blends fibers. *International Journal of Biological Macromolecules* 43(2): 106-114.
- Mawardi, I., Nurdin, N., Razak, H., Amalia, I., Sariyusda, S., Aljufri, A., Jaya, R.P. 2025. Development of lightweight engineered wood produced from derived sugarcane bagasse and coir fiber: Evaluation of the bending and thermal properties. *Journal of the Korean Wood Science and Technology* 53(1): 1-13.
- Moraes, M.A., Nogueira, G.M., Weska, R.F., Beppu, M.M. 2010. Preparation and characterization of insoluble silk fibroin/chitosan blend films. *Polymers* 2(4): 719-727.
- Nawawi, D.S., Maria, A., Firdaus, R.D., Rahayu, I.S., Fatrawana, A., Pramata, F., Sinaga, P.S., Friatiasari, W. 2023. Improvement of dimensional stability of tropical light-wood *Ceiba pentandra* (L) by combined alkali treatment and densification. *Journal of the Korean Wood Science and Technology* 51(2): 133-144.
- Negrea, P., Caunii, A., Sarac, I., Butnariu, M. 2015. The study of infrared spectrum of chitin and chitosan extract as potential sources of biomass. *Digest Journal of Nanomaterials & Biostructures* 10(4): 1129- 1138.
- Noishiki, Y., Nishiyama, Y., Wada, M., Kuga, S., Magoshi, J. 2002. Mechanical properties of silk fibroin-microcrystalline cellulose composite films. *Journal of Applied Polymer Science* 86(13): 3425-3429.
- Oh, S.Y., Yoo, D.I., Shin, Y., Kim, H.C., Kim, H.Y., Chung, Y.S., Park, W.H., Youk, J.H. 2005. Crystalline structure analysis of cellulose treated with sodium hydroxide and carbon dioxide by means of X-ray diffraction and FTIR spectroscopy. *Carbohydrate Research* 340(15): 2376-2391.
- Oliveira Barud, H.G., Barud, H.S., Cavicchioli, M., do Amaral, T.S., de Oliveira Junior, O.B., Santos, D.M., Petersen, A.L.O.A., Celes, F., Borges, V.M., de Oliveira, C.L., de Oliveira, P.F., Furtado, R.A., Tavares, D.C., Ribeiro, S.J.L. 2015. Preparation and characterization of a bacterial cellulose/silk fibroin sponge scaffold for tissue regeneration. *Carbohydrate Polymers* 128: 41-51.
- Ostadossein, F., Mahmoudi, N., Morales-Cid, G., Tamjid, E., Navas-Martos, F.J., Soriano-Cuadrado, B., Paniza, J.M.L., Simchi, A. 2015. Development of chitosan/bacterial cellulose composite films containing nanodiamonds as a potential flexible platform for wound dressing. *Materials* 8(9): 6401-6418.
- Park, K.C., Kim, B., Park, H., Park, S.Y. 2022. Peracetic acid treatment as an effective method to protect wood discoloration by UV light. *Journal of the Korean Wood Science and Technology* 50(4): 283-298.
- Park, N.H., Kim, D.H., Park, B., Jeong, E., Lee, J.W. 2013. The industry trend analysis and perspectives

- of biodegradable polymers. *Biomaterials Research* 17(3): 114-120.
- Perotto, G., Zhang, Y., Naskar, D., Patel, N., Kaplan, D.L., Kundu, S.C., Omenetto, F.G. 2017. The optical properties of regenerated silk fibroin films obtained from different sources. *Applied Physics Letters* 111(10): 103702.
- Plaza, G.R., Corsini, P., Pérez-Rigueiro, J., Marsano, E., Guinea, G.V., Elices, M. 2008. Effect of water on *Bombyx mori* regenerated silk fibers and its application in modifying their mechanical properties. *Journal of Applied Polymer Science* 109(3): 1793-1801.
- Rillig, M.C. 2012. Microplastic in terrestrial ecosystems and the soil? *Environmental Science & Technology* 46(12): 6453-6454.
- Santos, M.V., Santos, S.N.C., Martins, R.J., Almeida, J.M.P., Paula, K.T., Almeida, G.F.B., Ribeiro, S.J.L., Mendonça, C.R. 2019. Femtosecond direct laser writing of silk fibroin optical waveguides. *Journal of Materials Science: Materials in Electronics* 30(18): 16843-16848.
- Seo, Y.R., Kim, B.J. 2024. Fused filament fabrication of poly (lactic acid) reinforced with silane-treated cellulose fiber for 3D printing. *Journal of the Korean Wood Science and Technology* 52(3): 205-220.
- Setyayunita, T., Widyorini, R., Marsoem, S.N., Irawati, D. 2022. Effect of different conditions of sodium chloride treatment on the characteristics of kenaf fiber bundles. *Journal of the Korean Wood Science and Technology* 50(6): 392-403.
- Shang, S., Zhu, L., Fan, J. 2011. Physical properties of silk fibroin/cellulose blend films regenerated from the hydrophilic ionic liquid. *Carbohydrate Polymers* 86(2): 462-468.
- Sheavly, S.B., Register, K.M. 2007. Marine debris & plastics: Environmental concerns, sources, impacts and solutions. *Journal of Polymers and the Environment* 15(4): 301-305.
- Shih, C.M., Shieh, Y.T., Twu, Y.K. 2009. Preparation and characterization of cellulose/chitosan blend films. *Carbohydrate Polymers* 78(1): 169-174.
- Sionkowska, A. 2011. Current research on the blends of natural and synthetic polymers as new biomaterials: Review. *Progress in Polymer Science* 36(9): 1254-1276.
- Suryanto, H., Yanuhar, U., Wijaya, H.W., Binoj, J.S., Osman, A.F., Puspitasari, P., Maulana, J., Caesar, N.R., Nusantara, F., Komarudin, K. 2024. Synthesis and characterization of magnetic cellulose powder from sawdust waste. *Journal of the Korean Wood Science and Technology* 52(5): 504-523.
- Twu, Y.K., Huang, H.I., Chang, S.Y., Wang, S.L. 2003. Preparation and sorption activity of chitosan/cellulose blend beads. *Carbohydrate Polymers* 54(4): 425-430.
- Wang, B., Zhang, S., Wang, Y., Si, B., Cheng, D., Liu, L., Lu, Y. 2019. Regenerated *Antheraea pernyi* silk fibroin/poly(*N*-isopropylacrylamide) thermosensitive composite hydrogel with improved mechanical strength. *Polymers* 11(2): 302.
- Weng, R., Chen, L., Lin, S., Zhang, H., Wu, H., Liu, K., Cao, S., Huang, L. 2017. Preparation and characterization of antibacterial cellulose/chitosan nanofiltration membranes. *Polymers* 9(4): 116.
- Wu, T., Farnood, R., O'Kelly, K., Chen, B. 2014. Mechanical behavior of transparent nanofibrillar cellulose-chitosan nanocomposite films in dry and wet conditions. *Journal of the Mechanical Behavior of Biomedical Materials* 32: 279-286.
- Xu, Y.X., Kim, K.M., Hanna, M.A., Nag, D. 2005. Chitosan-starch composite film: Preparation and characterization. *Industrial Crops and Products* 21(2): 185-192.
- Yang, J., Kwon, G.J., Hwang, K., Byeon, J., Ghodake, G.S., Shinde, S.K., Hyun, S., Kim, D.Y. 2020. Influence of silk fibroin content on cellulose blend film using LiBr solution. *BioResources* 15(2): 2459-

- 2470.
- Yang, J., Kwon, G.J., Hwang, K., Kim, D.Y. 2018. Cellulose-chitosan antibacterial composite films prepared from LiBr solution. *Polymers* 10(10): 1058.
- Yang, J.Z., Liu, G.M., Sun, D.P. 2014a. Hemodialysis membrane prepared from bacterial cellulose/lithium chloride/N,N-dimethylacetamide solution. *Advanced Materials Research* 1048: 395-399.
- Yang, Y.J., Shin, J.M., Kang, T.H., Kimura, S., Wada, M., Kim, U.J. 2014b. Cellulose dissolution in aqueous lithium bromide solutions. *Cellulose* 21(3): 1175-1181.
- Yao, Y., Zhang, E., Xia, X., Yu, J., Wu, K., Zhang, Y., Wang, H. 2015. Morphology and properties of cellulose/silk fibroin blend fiber prepared with 1-butyl-3-methylimidazolium chloride as solvent. *Cellulose* 22(1): 625-635.
- Yasunaga, Y., Aso, Y., Yamada, K., Okahisa, Y. 2023. Preparation of transparent fibroin nanofibril-reinforced chitosan films with high toughness and thermal resistance. *Carbohydrate Polymer Technologies and Applications* 5: 100299.
- Zhang, M., Ding, C., Chen, L., Huang, L. 2014. The preparation of cellulose/collagen composite films using 1-ethyl-3-methylimidazolium acetate as a solvent. *BioResources* 9(1): 756-771.
- Zhang, Q., Li, M., Xu, W., Li, J., Yan, S. 2013. A novel silk fibroin scaffolds with oriented multichannels. *Materials Letters* 105: 8-11.
- Zhang, X., Xiao, N., Wang, H., Liu, C., Pan, X. 2018. Preparation and characterization of regenerated cellulose film from a solution in lithium bromide molten salt hydrate. *Polymers* 10(6): 614.
- Zhou, L., Wang, Q., Wen, J., Chen, X., Shao, Z. 2013. Preparation and characterization of transparent silk fibroin/cellulose blend films. *Polymer* 54(18): 5035-5042.